26th International Congress of Mechanical Engineering
COBEM 2021
ABCM Associação Brasileira de Engenharia e Ciências Mecânicas
November 22-26, 2021, Virtual Congress, Brazil

COB-2021-1612
Analysis and Modelling of Concentration Waves in Liquid-Solid Fluidized Beds in the Linear Regime

Victor Shumyatsky
University of Brasilia, Faculty of Technology, Department of Mechanical Engineering, Group of Fluid Mechanics of Complex Flows -VORTEX, Brasília, Brazil.
shumy2708@gmail.com

Yuri Dumaresq Sobral
University of Brasilia, Institute of Exact Sciences, Department of Mathematics and Group of Fluid Mechanics of Complex Flows -VORTEX, Brasília, Brazil.
ydsobral@unb.br

Francisco Ricardo da Cunha
University of Brasilia, Faculty of Technology, Department of Mechanical Engineering, Group of Fluid Mechanics of Complex Flows -VORTEX, Brasília, Brazil.
frcunha2@gmail.com

Abstract. *In this work, we investigate one-dimensional instabilities that occur in fluidized beds, focusing mainly on liquid-solid beds. The full set of averaged equations of motion for the continuous phases is used, as well as closure relations for the stress tensors of the fluid and solid phases and the interaction force between the phases. A linear stability analysis in the wavenumber space is performed in order to obtain the dispersion relation and the growth rate of small disturbances to the state of homogeneous fluidization. The influence of the physical parameters of the system, such as the Froude and Reynolds numbers, the density ratio between the phases on the stability of the bed is investigated. The effect of the particle pressure and particle viscosity on the bed stability is also examined. The results of this analysis are presented in terms of wave temporal growth rate and wave velocity as a function of wavenumber. In this way, the variation of one parameter while maintaining all other parameters fixed permits us to understand what physical mechanisms create instabilities in fluidized beds. In particular, we show the stabilizing effect that particle pressure and viscosity have on a fluidized bed and that high Froude number beds, despite having a narrow region of unstable modes, have large growth rates for high wavelength disturbances.*

Keywords: *Fluidized Beds, Linear stability, Concentration waves.*

1. INTRODUCTION

Consider a bed of solid particles in a tube that are supported by a perforated plate. Gas or liquid is forced to flow through the plate in the upward direction, with the condition that $\rho_s > \rho_f$, where ρ_s is the solid phase density, and ρ_f is the fluid phase density. At low flow rates, the bed is packed at the bottom of the tube and the fluid flows through it as if it was a porous medium. As the flow rate increases, a small expansion of the bed starts to occur when the drag exerted by the fluid on the particles balances their weight corrected for buoyancy. Onwards, any further increase of the flow rate causes the bed to expand, and it is said to be fluidized, because the particles behave like a new fluid. The flow rate at which the bed starts to expand is denoted by q_{mf}.

Fluidized beds are widely used in the industry for chemical processes or transformations, due to the high rates of mass and heat transfer that can be obtained because of the intense interaction between fluid and particles. Hence, research of the physics of fluidized beds is important in the chemical engineering science.

Fluidized beds are long known to be susceptible to the propagation of instabilities, such as bubbles (usually in gas-solid beds) and traveling concentration waves (usually in liquid-solid beds). These instabilities have proven to be a fascinating topic of research, and there still are many unanswered questions about them and the physical mechanisms that governate them.

The problem of fluidized bed stability has a long history. Initially, a criteria of bed stability based on the Froude number based on the minimum fluidization velocity, defined by $Fr_{mf} = u_{mf}^2/gd_s$, where u_{mf} is the velocity of minimum fluidization of the bed, g is the acceleration of gravity and d_s is the diameter of the solid particles, was proposed in Wilhelm and Kwauk (1948). In that work, based on experimental results, the authors concluded that when $Fr \ll 1$, the bed showed a non-bubbling behavior. Subsequent research showed that the fluidized bed dynamics are more complex than the classification proposed in Wilhelm and Kwauk (1948).

(Anderson and Jackson, 1967) was a pioneering work in the mathematical modelling of fluidized beds. The main idea of that paper was to use averaging techniques to obtain mean variables and, thus, obtain averaged equations of motion that treat both phases as continua. This enables us to solve the set of partial differential equations of motion for both phases, instead of solving equations of motion for each particle independently, which can be very costly. To fully close the set of averaged equations of motion, one needs closure relations for the stress tensors and the interaction force between the phases. These closure relations can be based on experimental and phenomenological arguments, but have to be chosen carefully so that no physical mechanism is overlooked. The uncertainty in this unknown terms is one of the major drawbacks of this two fluid continuum description. Linear stability analysis are performed imposing small wave perturbations to an equilibrium solution of the set of equations of motion, thus linearizing them and obtaining the growth rate of the disturbance.

The physical mechanism behind the instabilities was understood with the work (Jackson, 1963), which explained that the particle inertia causes relative velocities between fluid and the disperse phase, thus creating regions of voidage and regions of higher concentration of particles that propagate throughout the bed. The linear stability analysis performed in that work stated that fluidized beds are always unstable, which is not true. Some years later, the work (Garg and Pritchett, 1975) showed that the particle pressure is the key to stabilize a fluidized bed, and if it is sufficiently large, instabilities will be dissipated. Since then, in many more works, such as (Batchelor, 1988) and (Anderson *et al.*, 1995), the physics of instabilities in fluidized beds have been investigated.

Instabilities grow much faster in gas-solid fluidized beds than in liquid-solid fluidized beds, due to the big difference in density between gas and the particles (Sundaresan, 2003). However, liquid-solid systems show propagation of one-dimensional concentration waves, which are very useful particulate flows for understanding fluidized bed dynamics.

In this paper, using a simple reliable model for the physics of a liquid-solid fluidized bed, we examine a fluidized bed stability to the propagation of a plane one-dimensional concentration wave, identifying the relevant nondimensional parameters and physical mechanisms that affect the onset and the growth rate of this kind of instabilities.

2. FORMULATION OF THE PROBLEM

The governing equations used in this work can be obtained through the averaging procedure presented in the classical paper of Anderson and Jackson (1967). Applying the same method to the equations of conservation of mass and momentum equations of both the liquid and the solid phases, we obtain the following set of averaged equations:

$$\frac{\partial \epsilon}{\partial t} + \nabla \cdot (\epsilon \boldsymbol{u}) = 0, \tag{1}$$

$$\frac{\partial \phi}{\partial t} + \nabla \cdot (\phi \boldsymbol{v}) = 0, \tag{2}$$

$$\epsilon \rho_f \frac{D\boldsymbol{u}}{Dt} = \nabla \cdot (\boldsymbol{T_f}) - \boldsymbol{f} + \epsilon \rho_f \boldsymbol{b}, \tag{3}$$

$$\phi \rho_s \frac{D\boldsymbol{v}}{Dt} = \nabla \cdot (\boldsymbol{T_s}) + \boldsymbol{f} + \phi \rho_s \boldsymbol{b}, \tag{4}$$

where $\phi(\boldsymbol{x}, t)$ is the local particle concentration, $\epsilon = 1 - \phi$ is the voidage fraction, $\boldsymbol{u}(\boldsymbol{x}, t)$ and $\boldsymbol{v}(\boldsymbol{x}, t)$ are the fluid and solid phases velocities, respectively. Here, $\boldsymbol{T_f}$ is the fluid mean stress tensor, $\boldsymbol{T_s}$ is the particle mean stress tensor, $\boldsymbol{f}$ is the interaction force between the phases, and $\boldsymbol{b}$ is the total body force acting on the phases (in this work, $\boldsymbol{b}$=$\boldsymbol{g}$, the acceleration of gravity, but it can also incorporate magnetic or electric forces, for instance). Equations (1) and (2) represent the balance of mass for the fluid phase and solid phase, respectively, whereas equations (3) and (4) represent the balance of momentum for the liquid phase and solid phase, respectively. The stress tensors are defined to have a simple Newtonian fluid-like form:

$$\boldsymbol{T_f} = -p\boldsymbol{I} + \mu_f \left[\nabla \boldsymbol{u} + \nabla \boldsymbol{u}^T - \frac{2}{3}(\nabla . \boldsymbol{u})\boldsymbol{I} \right], \tag{5}$$

and

$$\boldsymbol{T_s} = -p_s(\phi)\boldsymbol{I} + \mu_s(\phi) \left[\nabla \boldsymbol{v} + \nabla \boldsymbol{v}^T - \frac{2}{3}(\nabla . \boldsymbol{v})\boldsymbol{I} \right], \tag{6}$$

for the fluid and solid phases, respectively. The viscosity , μ, and the pressure of the fluid phase, p, are defined as usual, whereas the particle pressure, $p_s(\phi)$, and viscosity, $\mu_s(\phi)$, both account for the mean effect of collisions and velocity fluctuations of the particles, and are functions of the particle volume fraction. Several closure relations for the particle pressure and viscosity have been used throughout the years. In this work, we use the following expression for the particle viscosity:

$$\mu_s(\phi) = 0.18\frac{\rho_s d_s v_t}{\phi_{rlp} - \phi}, \tag{7}$$

where v_t is the terminal settling velocity of the particles and ϕ_{rlp} is the random loose packing concentration, measured experimentally. Equation (7) was obtained experimentally by Duru *et al.* (2002) for the range of parameters used in that work. For the particle pressure, we use the ad-hoc model proposed in Hernández and Jimenez (1991):

$$p_s(\phi) = \tau\phi^3 exp\left(\frac{r\phi}{\phi_{cp} - \phi}\right), \tag{8}$$

where ϕ_{cp} is the close packing concentration and τ and r are constants of the model that need to be chosen carefully if one is willing to reproduce numerically experimental results. In addition, it should be important to note that the bed mean flow rate, q, is trivially related to the fluid and solid phase velocities by

$$q = \phi v + (1 - \phi)u. \tag{9}$$

An important experimental correlation between the mean flow rate, q and the homogeneous volume fraction of the bed, ϕ_0, which can be defined as the total volume of particles divided by the total bed volume, was obtained by Richardson and Zaki (1954):

$$q = v_t(1 - \phi_0)^n, \tag{10}$$

where the exponent n is measured experimentally. To fully close the set of governing equations, a constitutive relation for the interaction force between the phases is also needed. Additionally, we use a simple model for the interaction force:

$$\boldsymbol{f} = \rho_f \hat{c}(\phi)\left(\frac{\partial \boldsymbol{u}}{\partial t} - \frac{\partial \boldsymbol{v}}{\partial t}\right) + \beta(\phi)(\boldsymbol{u} - \boldsymbol{v}). \tag{11}$$

The first term of the right-hand side of Eq.(11) denotes the added mass force, which is important in liquid-solid fluidized beds and the second term of the right-hand side denotes a linear viscous drag force of the fluid on the particles. For the added mass coefficient, we use a simple expression suggested in the work by Sobral and Hinch (2017):

$$\hat{c}(\phi) = \frac{1}{2}\frac{1}{1 - \phi}. \tag{12}$$

The viscous drag coefficient, $\beta(\phi)$, is also a function of the particle volume fraction. Using the Richardson-Zaki correlation, Eq.(10), and considering that at minimum fluidization the drag force roughly balances the weight of the particles, the following expression for $\beta(\phi)$ can be derived:

$$\beta(\phi) = \frac{\rho_s g}{v_t}\frac{\phi}{(1 - \phi)^{n-1}}, \tag{13}$$

From this point, we restrict our attention to one-dimensional and unsteady disturbances. Hence, the set of governing equations in one dimension is given by:

$$-\frac{\partial \phi}{\partial t} + \frac{\partial}{\partial x}\left[(1 - \phi)u\right] = 0, \tag{14}$$

$$\frac{\partial \phi}{\partial t} + \frac{\partial}{\partial x}(\phi v) = 0, \tag{15}$$

$$(1 - \phi)\rho_f\left(\frac{\partial u}{\partial t} + u\frac{\partial u}{\partial x}\right) + \rho_f \hat{c}(\phi)\left(\frac{\partial u}{\partial t} - \frac{\partial v}{\partial t}\right) = -\frac{\partial p}{\partial x} + \frac{4\mu_f}{3}\frac{\partial^2 u}{\partial x^2} - \beta(\phi)\left(u - v\right) - (1 - \phi)\rho_f g. \tag{16}$$

$$\phi\rho_s\left(\frac{\partial v}{\partial t}+v\frac{\partial v}{\partial x}\right)-\rho_f\hat{c}(\phi)\left(\frac{\partial u}{\partial t}-\frac{\partial v}{\partial t}\right)=-\frac{\partial p_s}{\partial x}+\frac{4}{3}\frac{\partial}{\partial x}\left(\mu_s\frac{\partial v}{\partial x}\right)+\beta(\phi)\left(u-v\right)-\phi\rho_s g, \tag{17}$$

In order to understand the physical mechanisms involved in fluidized beds dynamics, we define typical scales of the two-phase flow system. We use the terminal velocity v_t as a velocity scale, d_s as the length scale, μ_f as a viscosity scale and $\rho_f v_t^2$ as a pressure scale. Time is scaled with d_s/v_t. Applying the scalings above, we obtain the following nondimensional momentum equations for the fluid and the solid phases, respectively:

$$(1-\phi)\left(\frac{\partial u^*}{\partial t^*}+u\frac{\partial u^*}{\partial x^*}\right)+\hat{c}(\phi)\frac{\partial(u^*-v^*)}{\partial t^*}=-\frac{\partial p^*}{\partial x^*}+\frac{4}{3Re}\frac{\partial^2 u^*}{\partial x^{*2}}-\frac{\beta^*(\phi)}{R_\rho Fr}\left(u^*-v^*\right)-\frac{(1-\phi)}{Fr}, \tag{18}$$

$$\phi\left(\frac{\partial v^*}{\partial t^*}+v^*\frac{\partial v^*}{\partial x^*}\right)-R_\rho\hat{c}(\phi)\frac{\partial(u^*-v^*)}{\partial t^*}=-R_\rho\frac{\partial p_s^*}{\partial x^*}+\frac{4R_\rho}{3Re}\frac{\partial}{\partial x^*}\left(\mu_s^*\frac{\partial v^*}{\partial x^*}\right)+\frac{\beta^*(\phi)}{Fr}\left(u^*-v^*\right)-\frac{\phi}{Fr}, \tag{19}$$

where asterisk denotes nondimensional variables. From Eq.(13),we can write the nondimensional drag coefficient $\beta^*(\phi)$ as follows:

$$\beta^*(\phi)=\frac{\phi}{(1-\phi)^{n-1}}. \tag{20}$$

From this point, in order to make the notation as simple as possible, all variables are assumed to be nondimensional and the asterisk will no longer be used. The continuity equations, Eqs.(14), (15) are still valid, considering now time, t, and space, x, to be nondimensional. In Eqs.(19) and (18), we identify the following important nondimensional parameters:

$$R_\rho=\frac{\rho_f}{\rho_s},\quad Fr=\frac{v_t^2}{gd_s},\quad Re=\frac{\rho_f d_s v_t}{\mu_f}. \tag{21}$$

The density ratio, R_ρ, is a fundamental parameter of fluidized beds, and, as we will see, strongly affects bed stability. The Froude numbe, Fr, measures the relative importance between the inertial and gravitational forces acting on the bed, and the Reynolds number, Re, measures the relative importance between inertial and viscous forces.

3. LINEAR STABILITY ANALYSIS

The set of governing equations admits an equilibrium solution, namely:

$$\begin{cases}\phi=\phi_0\\ u=u_0\\ v=0\\ p=p_0\end{cases}, \tag{22}$$

where the Richardson-Zaki correlation implies that $u_0=(1-\phi_0)^{(n-1)}$. From Eq.(18), it follows that $\partial p_0/\partial x$ is given by:

$$\frac{\partial p_0}{\partial x}=\frac{(R_\rho-1)\phi_0-R_\rho}{R_\rho Fr} \tag{23}$$

This equilibrium solution is called homeogeneous state. Now, in order to examine the bed stability, we linearize the set of governing equations around the homogeneous state by imposing small amplitude perturbations:

$$\phi=\phi_0+\phi_1,\quad u=u_0+u_1,\quad v=v_1,\quad p=p_0+p_1. \tag{24}$$

Thus, we obtain the following system of equations for the perturbation variables:

$$-\frac{\partial\phi_1}{\partial t}+(1-\phi_0)\frac{\partial u_1}{\partial x}-u_0\frac{\partial\phi_1}{\partial x}=0, \tag{25}$$

$$\frac{\partial \phi_1}{\partial t} + \phi_0 \frac{\partial v_1}{\partial x} = 0, \tag{26}$$

$$\phi_0 \frac{\partial v_1}{\partial t} - R_\rho \hat{c}(\phi) \left(\frac{\partial u_1}{\partial t} - \frac{\partial v_1}{\partial t} \right) = -R_\rho \frac{dp_s}{d\phi}(\phi_0) \frac{\partial \phi_1}{\partial x} + \frac{4R_\rho \mu_s(\phi_0)}{3Re} \frac{\partial^2 v_1}{\partial x^2} + \frac{\beta(\phi_0)}{Fr}(u_1 - v_1) + \frac{\beta'(\phi_0) u_0 \phi_1}{Fr} - \frac{\phi_1}{Fr}, \tag{27}$$

$$(1-\phi_0) \left(\frac{\partial u_1}{\partial t} + u_0 \frac{\partial u_1}{\partial x} \right) + \hat{c}(\phi) \left(\frac{\partial u_1}{\partial t} - \frac{\partial v_1}{\partial t} \right) = -\frac{\partial p_1}{\partial x} + \frac{4}{3Re} \frac{\partial^2 u_1}{\partial x^2} - \frac{\beta(\phi_0)}{R_\rho Fr}(u_1 - v_1) - \frac{\beta'(\phi_0) u_0 \phi_1}{R_\rho Fr} + \frac{\phi_1}{Fr}, \tag{28}$$

where $\beta'(\phi)$ denotes the derivative of the drag coefficient with respect to particle concentration. Imposing that the small perturbations have a plane wave form:

$$\phi_1 = \phi_a e^{i(kx-st)}, \quad u_1 = u_a e^{i(kx-st)}, \quad v_1 = v_a e^{i(kx-st)}, \quad p_1 = p_a e^{i(kx-st)}, \tag{29}$$

where k denotes the wave number and s the frequency of the disturbances, we rewrite our set of governing equations as a linear system of the form

$$\boldsymbol{Ml} = \boldsymbol{0}. \tag{30}$$

In Eq. (30), the vector $\boldsymbol{l}$ contains the amplitudes of the perturbations, and is given by

$$\boldsymbol{l} = \begin{pmatrix} \phi_a \\ v_a \\ u_a \\ p_a \end{pmatrix}, \tag{31}$$

whereas the coefficient matrix $\boldsymbol{M}$ represents a linear transformation from the physical space $(x-t)$ to the reciprocal space $(k-\omega)$ and is given by:

$$\boldsymbol{M} = \begin{pmatrix} -s & \phi_0 k & 0 & 0 \\ s - u_0 k & 0 & (1-\phi_0)k & 0 \\ A & B & C & 0 \\ D & E & F & ik \end{pmatrix}. \tag{32}$$

Here, the components A, B, C, D, E and F are defined as follows:

$$\begin{aligned}
A &= R_\rho \frac{dp_s}{d\phi}(\phi_0) ik - \frac{1}{Fr}[\beta'(\phi_0) u_0 - 1], \\
B &= -\phi_0 is - R_\rho \hat{c}(\phi_0) is + \frac{4R_\rho}{3Re} \mu_s(\phi_0) k^2 + \frac{\beta(\phi_0)}{Fr}, \\
C &= R_\rho \hat{c}(\phi_0) is - \frac{\beta(\phi_0)}{Fr}, \\
D &= \frac{\beta'(\phi_0) u_0}{R_\rho Fr} - \frac{1}{Fr}, \\
E &= \hat{c}(\phi_0) is - \frac{\beta(\phi_0)}{R_\rho Fr}, \\
F &= (1-\phi_0) i(u_0 k - s) - \hat{c}(\phi_0) is + \frac{4k^2}{3Re} + \frac{\beta(\phi_0)}{R_\rho Fr}.
\end{aligned} \tag{33}$$

For the homogeneous system given in Eq. (30) to have a nontrivial solution, it must satisfy the condition

$$det(\boldsymbol{M}) = 0. \tag{34}$$

Now, in order to examine the temporal evolution of the disturbances at their initial, linear phase, we impose a complex frequency of the form $s = \omega + \xi_s i$.

$$e^{i(kx-st)} = e^{\xi_s t} e^{i(kx-\omega t)} \tag{35}$$

By doing so, Eq.(35) shows that the real part of the complex frequency, ω, is the frequency of the propagating modes and $\omega = \omega(k)$ is the dispersion relation of the waves, whereas the complex part of the frequency, ξ_s, is the growth rate of the disturbances. Expanding Eq.(34), we obtain we obtain the following characteristic equation of this eigenvalues-eingenmodes problem:

$$B_1(k)s^2 + B_2(k)s + B_3(k) = 0, \tag{36}$$

where $B_1 = B_{1i}i + B_{1r}$, $B_2 = B_{2i}i + B_{2r}$, $B_3 = B_{3i}i + B_{3r}$ are all complex coefficients and are combinations of the elements of $\boldsymbol{M}$. Solving equation (36) for s, we thus determine the dispersion relation and the growth rate of the disturbances. The results for the particulate flow explored here will be presented in Section 4.

4. RESULTS AND DISCUSSION

In this section, results of the growth rate and the velocity of the disturbances as a function of the wavenumber, k, are presented. We set the same values of dimensional quantites used in a numerical simulation work performed by Sobral and Hinch (2017), and also previously in the experiments carried out by Duru *et al.* (2002). In this way, we guarantee that the parameters here used are meaningful and represent actual physics of a fluidized bed. Adapting their dimensional quantities to our nondimensional physical parameters, we find:

$$Fr = 4, \quad Re = 120, \quad R_\rho = 0.25, \quad \tau = 2.48 \times 10^{-3}, \quad \phi_0 = 0.549, \quad \phi_{cp} = 0.612, \quad \phi_{rlp} = 0.58. \tag{37}$$

The set of nondimensional parameters Eq.(37) is used in all of the results of this section, unless stated otherwise. It is worth to note that the linearization of the governing equations around the equilibrium state, ϕ_0, means that the actual dependence of all the material or flow functions of the particle volume fraction, such as the particle pressure, the particle viscosity and the drag and added mass coefficients, is not relevant for the linear stability analysis. Instead, the value of these functions evaluated only on the homogeneous particle volume fraction ϕ_0 is considered in a linear regime of the bed stability. Therefore, to simplify our notation, for this analysis, we define:

$$\frac{dp_s}{d\phi}(\phi_0) \equiv \sigma, \quad \mu_s(\phi_0) \equiv \hat{M}. \tag{38}$$

The corresponding values of these two parameters used by Sobral and Hinch (2017), were: $\sigma = 0.29$ and $\hat{M} = 3000$.

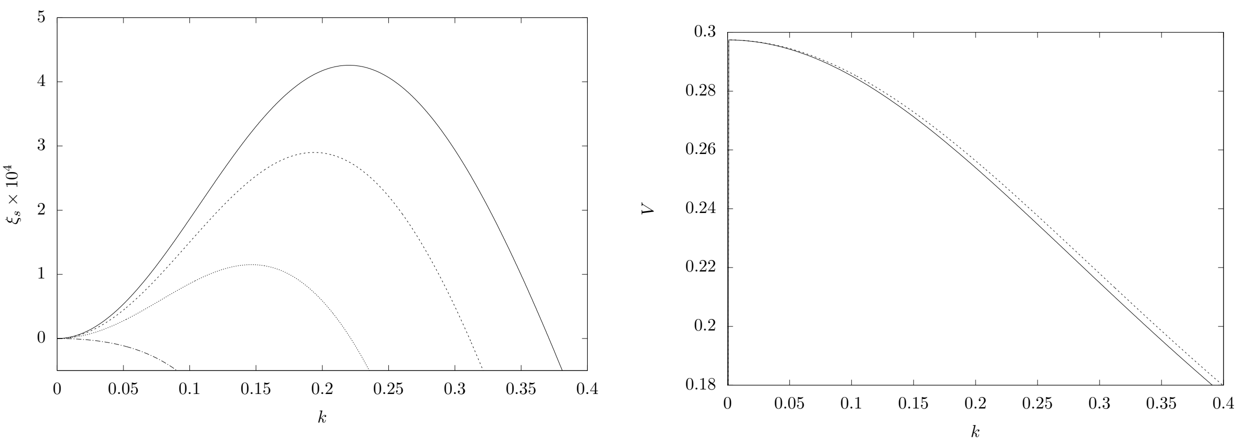

(a) Growth rate of plane waves for several values of σ. Solid line: $\sigma = 0.15$; dashed line: $\sigma = 0.20$; dotted line: $\sigma = 0.29$; dash-dotted line: $\sigma = 0.50$.

(b) Comparison between wave velocities for $\sigma = 0.1$ (solid line) and $\sigma = 5.0$ (dashed line).

Figure 1: Influence of particle pressure mechanisms on bed stability.

Equation (35) shows that when the growth rate of the disturbances, ξ_s, is positive, the amplitude of the disturbances grows, whereas when ξ_s is negative, the amplitude decays and the waves are dissipated throughout the bed. From the dispersion relation found through Eq.(36), we can also obtain the velocity of the propagating modes, which is given by $V = \omega/k$. The influence of the parameters σ, $\hat{M}$, R_ρ and Fr on bed stability and on the velocity of the modes will be examined below.

As already mentioned, in the theoretical work developed by Garg and Pritchett (1975), it was established that the mechanism associated with particle pressure are responsible for the stabilization of fluidized beds. First, the value of the derivative of the particle pressure with respect to particle volume fraction evaluated at the homogeneous state, σ, is varied, while all other parameters remain fixed. It is important to recall that the wavelength of the disturbances, λ, is related to the wavenumber through the simple expression $\lambda = 2\pi/k$. Figure 1(a) shows that modes with sufficiently large wavenumbers (or small wavelenghts) have negative growth rates, and therefore are stable. As expected, bed stability is strongly influenced by σ. As σ increases, the range of modes with positive growth rate gets considerably narrower, and the maximum value of growth rate also decreases. For a sufficiently big σ, all the modes have negative growth rates and the bed is entirely stable.

The particle pressure owes its existence to particle-particle interactions, such as collisions and momentum transfer through velocity fluctuations. Thus, it is expected to generate a diffusive mechanism in the bed, dissipating higher concentration regions. If this effect is strong enough, it should be sufficient to dissipate the propagation of concentration waves, which is exactly what the results presented in Fig. 1(a) have pointed out. From Fig. 1(b), it follows that modes with larger wavenumbers, and therefore, smaller wavelengths, which we can call short waves, propagate with smaller velocities. In general, the waves that are observed in real life fluidized beds are those with larger wavelenghts and velocities, or long waves. It is still interesting to observe from Figure 1(b) that the particle pressure in linear regimes barely affects the velocity of the modes, despite having a remarkable effect on the overall bed stability, as discussed earlier. We can see that even with the largest value of σ tested here, $\sigma = 5$, which is by far enough to stabilize all the modes, the velocities of the modes are practically the same as for a moderate value of $\sigma = 0.1$. However, it is seen that the propagation velocities of short waves are slightly influenced by the particle pressure parameter. The results suggest that in a typical liquid-solid bed the volumetric expansion of structures like particles aggregates formed along the bed has just a small influence on the short and long waves velocities.

Next, we examine the effect of the particle viscosity on bed stability. As the particle pressure, the particle viscosity accounts for momentum diffusion due to velocity fluctuations in the solid phase, and we will show that this parameter has a strong effect on the short waves. The mechanism of particle viscosity in the bed also incorporates the effect of resistance of the fluid (i.e. a extra production of internal energy in the suspension due to the stresslet of the particle exerced on the fluid) to change of particle configuration, due to viscous stresses (Batchelor, 1988). It is worth noting that in Eq.(19), $\hat{M}$ is multiplied by the Reynolds number, that compares the he relative importance of inertial mechanisms with viscous ones. Therefore, changing $\hat{M}$ is analogous to vary Re in a way that the product between them is the same. Owing to the dissipative nature of the particle viscosity, it is expected that, as it gets larger, the range of unstable modes gets smaller.

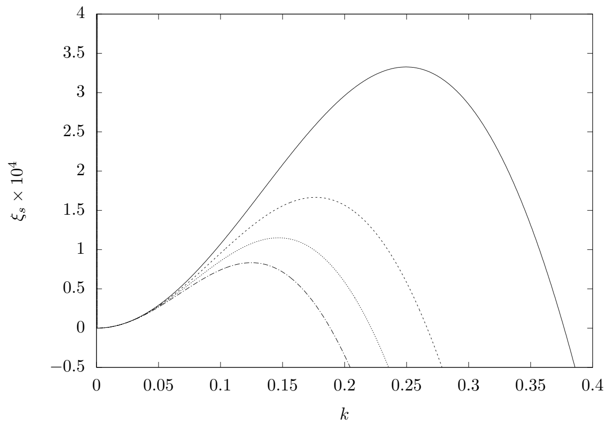

(a) Growth rate of plane waves for several values of $\hat{M}$. Solid line: $\hat{M} = 1000$; dashed line: $\hat{M} = 2000$; dotted line: $\hat{M} = 3000$; dash-dotted line: $\hat{M} = 4000$.

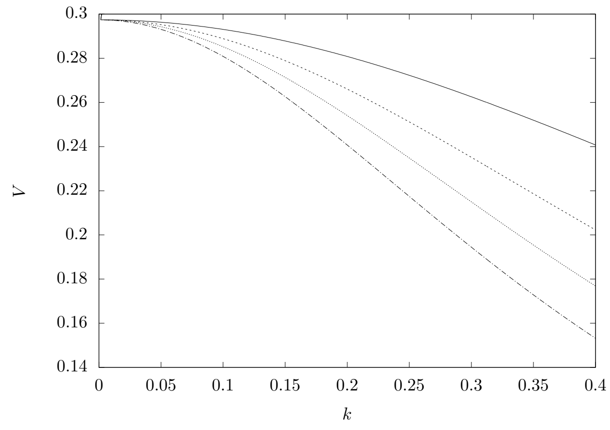

(b) Comparison between wave velocities for some values of $\hat{M}$. Solid line: $\hat{M} = 1000$; dashed line: $\hat{M} = 2000$; dotted line: $\hat{M} = 3000$; dash-dotted line: $\hat{M} = 4000$.

Figure 2: Influence of particle viscosity mechanisms on bed stability.

This behavior can be clearly identified in Fig. 2(a), where the variation of $\hat{M}$ strongly affects the instability onset, as well as the maximum possible growth rate. In addition, we see that the effect of particle viscosity works as a filter for large wavenumbers, attenuating to zero the disturbances corresponding to short waves for a given value of the parameter $\hat{M}$. In contrast with the effect that the particle pressure mechanism has on the velocity of the modes, Fig. 2(b) shows that the particle viscosity considerably affects the propagation velocity of the waves. The dissipative nature of the viscosity brings with it a dampening effect on the disturbances. Hence, the particle viscosity works to reduce wave amplitude and also its propagation velocity.

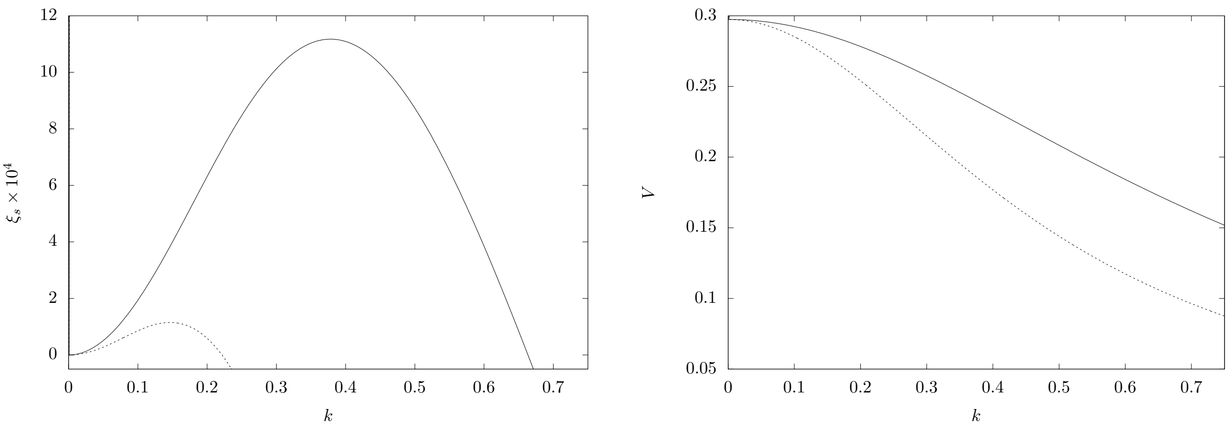

(a) Growth rate of plane waves for $R_\rho = 0.1$ (solid line) and $R_\rho = 0.25$ (dashed line).

(b) Comparison between wave velocities for $R_\rho = 0.1$ (solid line) and $R_\rho = 0.25$ (dashed line).

Figure 3: Influence of the ratio of densities on the bed stability.

A crucial parameter of a fluidized bed is the ratio of densities, R_ρ. As for fluidization to occur, ρ_s must be greater than ρ_f, it follows that R_ρ has a value between 0 and 1. Gas-solid fluidized beds typically have values of R_ρ of the order of $1/100$, while liquid-solid fluidized beds ratios of densities are at least an order of magnitude greater. This work focuses on liquid-solid fluidized beds. As mentioned earlier, gas-solid beds commonly exhibit the presence of bubbles. It has long been speculated (Batchelor, 1993) that this bubbling regime is consequence of a two-dimensional destabilization of one-dimensional concentration waves. Fig. 3(a) shows that for $R_\rho = 0.1$, a value still standard for liquid-solid beds, the maximum growth rate is roughly 10 times greater than the maximum growth rate for $R_\rho = 0.25$. The range of unstable modes is also significantly smaller for $R_\rho = 0.25$. This behavior of the model fully agrees with the fact that gas-solid beds are much more unstable than liquid ones, and hints that bubbling regimes and the secondary instability that creates them may occur due to the very fast growth of disturbances in gas-solid beds. Figure 3(b) also shows that R_ρ significantly affects the propagation velocities of waves in a fluidized bed, with smaller values of ratio of densities meaning faster propagation of disturbances.

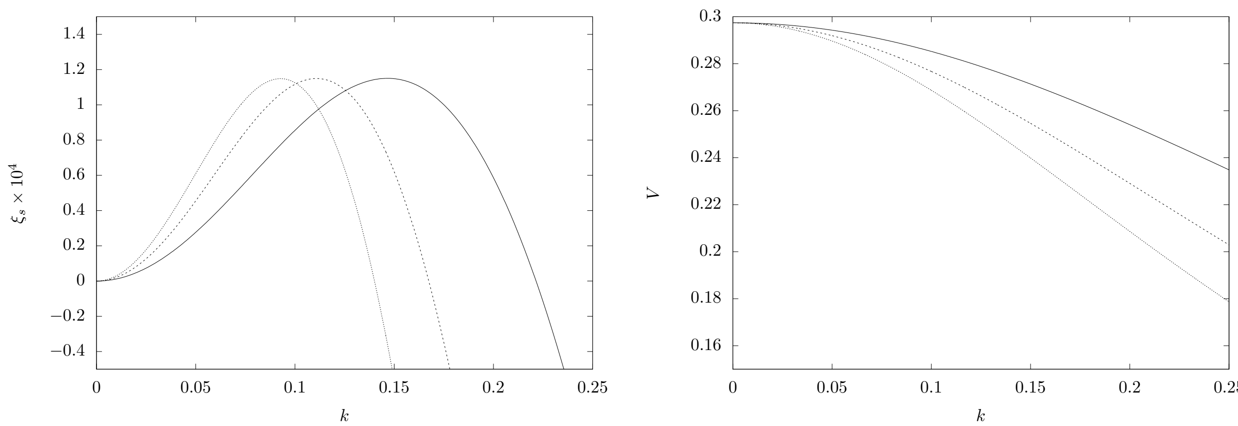

(a) Growth rate of plane waves for $Fr = 4$ (solid line), $Fr = 7$ (dashed line) and $Fr = 10$ (dotted line).

(b) Comparison between wave velocities for $Fr = 4$ (solid line), $Fr = 7$ (dashed line) and $Fr = 10$ (dotted line) .

Figure 4: Influence of the Froude number on bed stability.

The Froude number, Fr, is also an important parameter to characterize the dynamics of a fluidized bed. It compares the relative importance of inertial forces with the gravitational forces. Inertia is fundamentally responsible for the presence of instabilities in fluidized beds, because of the delay of the particles to follow the flow of the fluid, hence creating relative velocities between particles and fluid. Thus, one would expect that beds with high Fr numbers are more unstable than beds with low Fr numbers. The results shown in Fig. 4(a) may at first seem counter-intuitive. Beds with higher Fr numbers showed a narrower range of unstable modes. Varying Fr barely affected the maximum growth rate of the disturbances, in contrast with the dissipative effect of $\hat{M}$ discussed in Fig. 2(a). Increasing Fr also reduced the propagation velocities of the waves, as shown in Fig. 4(b), which is a direct consequence of the wider distribution of modes that occurs for lower Fr beds. However, it is quite interesting to note that with the physical model explored in this work, larger values of Fr

indicate that waves with higher wavelengths (long waves) will have the maximum rate of amplification, characterizing an inertial regime of long waves of small amplitude. Figura 4a suggests, for instance, that for a fixed value of a large wavelength, namely, $\lambda = 20\pi$, correspondent to an wavenumber of $k = 0.1$, the disturbance corresponding to the higher Fr will have the larger rate of amplification.

So, the linear analysis here is indeed predicting a more unstable configutation with maximum growth rate occuring in the regime of long waves for higher values of Froude. In particular, the long wave scale (i.e. small k) dominates the instability of the bed at higher values of Fr.

5. CONCLUSIONS

In this work, we investigated the influence of different physical mechanisms in fluidized beds on the overall bed stability to the propagation of one-dimensional concentration waves. The results showed the stabilizing effect of the particle pressure and the particle viscosity, due to their dissipative of high concentration regions nature. Also, the behavior of the particle viscosity as a filter of short waves was observed, as well as its strong influence on the velocities of the propagating modes. Fluidized beds with lower values of ratio of densities proved to be far more unstable and have much faster propagating waves that beds with higher values of ratio of densities, as expected. The influence of the Froude number on bed stability showed some interesting results. They indicate that high Froude number beds have a narrower region of unstable modes than low Froude number beds, which at first may seem counterintuitive. On the other hand, high Froude number beds have higher growth rate of disturbances than low Froude number beds, if we fix one mode with same wavelength that is unstable for both beds. Thus, the results indicate that the inertial effects that occur in high Fr beds imply the propagation of long and more unstable waves, with the maximum growth rate mode having a larger wavelength than the wavelength of the maximum growth rate mode of a lower Fr bed. When non-linearities take over at some point of the wave evolution, it may well be that long waves that propagate in high Fr beds would become faster than those that propagate for low values of Fr, thus further corroborating the fact that in experiments, higher Froude number beds tend to be more unstable. In future works, it would be promising to compare results of the linear stability analysis here performed with numerical simulations of the governing equations, aiming to understand how the parameters affect not only the linear phase of the growth of disturbances, but also their full time evolution.

6. ACKNOWLEDGEMENTS

The authors would like to thank the Brazilian Coordination of Superior Level Staff Improvement-CAPES and the Brazilian National Council for Scientific and Technological Development - CNPq (Grants n. 310399/2020-3 and 421177/2018-7; 131557/2020-3.) for the financial support throughout the development of this work.

7. REFERENCES

Anderson, K., Sundaresan, S. and Jackson, R., 1995. "Instabilities and the formation of bubbles in fluidized beds". *Journal of Fluid Mechanics*, Vol. 303, pp. 327–366.

Anderson, T.B. and Jackson, R., 1967. "Fluid mechanical description of fluidized beds. equations of motion". *Industrial & Engineering Chemistry Fundamentals*, Vol. 6, No. 4, pp. 527–539.

Batchelor, G., 1988. "A new theory of the instability of a uniform fluidized bed". *Journal of Fluid Mechanics*, Vol. 193, pp. 75–110.

Batchelor, G., 1993. "Secondary instability of a gas-fluidized bed". *Journal of Fluid Mechanics*, Vol. 257, pp. 359–371.

Duru, P., Nicolas, M., Hinch, J. and Guazzelli, E., 2002. "Constitutive laws in liquid-fluidized beds". *Journal of Fluid Mechanics*, Vol. 452, pp. 371–404.

Garg, S. and Pritchett, J., 1975. "Dynamics of gas-fluidized beds". *Journal of Applied Physics*, Vol. 46, No. 10, pp. 4493–4500.

Hernández, J.A. and Jimenez, J., 1991. "Bubble formation in dense fluidised beds". In *The Global Geometry of Turbulence*, Springer, pp. 133–142.

Jackson, R., 1963. "The mechanics of fluidized beds. i. the stability of the state of uniform fluidization". *Trans. Inst. Chem. Engrs.*, Vol. 41, pp. 13–21.

Richardson, J. and Zaki, W., 1954. "The sedimentation of a suspension of uniform spheres under conditions of viscous flow". *Chemical Engineering Science*, Vol. 3, No. 2, pp. 65–73.

Sobral, Y.D. and Hinch, E.J., 2017. "Finite amplitude steady-state one-dimensional waves in fluidized beds". *SIAM Journal on Applied Mathematics*, Vol. 77, No. 1, pp. 247–266.

Sundaresan, S., 2003. "Instabilities in fluidized beds". *Annual review of fluid mechanics*, Vol. 35, No. 1, pp. 63–88.

Wilhelm, R. and Kwauk, M., 1948. "Fluidization of solid particles". *Chem. Eng. Prog.*, Vol. 44, pp. 201–218.

8. RESPONSIBILITY NOTICE

The authors are solely responsible for the printed material included in this paper.